the plant journal

SEB SOCIETY FOR EXPERIMENTAL BIOLOGY

The Plant Journal (2022) **111,** 731–747 doi: 10.1111/tpj.15847

The terminal enzymatic step in piperine biosynthesis is co-localized with the product piperine in specialized cells of black pepper (*Piper nigrum* L.)

Luise Jäckel[1], Arianne Schnabel[1], Hagen Stellmach[1], Ulrike Klauß[1], Susanne Matschi[2], Gerd Hause[3] and Thomas Vogt[1,*]

[1]*Department of Cell and Metabolic Biology, Leibniz Institute of Plant Biochemistry, Weinberg 3, D-06120, Halle (Saale), Germany,*
[2]*Department of Biochemistry of Plant Interactions, Leibniz Institute of Plant Biochemistry, Weinberg 3, D-06120, Halle (Saale), Germany, and*
[3]*Electron Microscopy Lab, Biocenter, Martin-Luther-University Halle-Wittenberg, Weinbergweg 22, D-06120, Halle (Saale), Germany*

Received 15 March 2022; revised 18 May 2022; accepted 26 May 2022.; published online 30 May 2022.
*For correspondence (e-mail tvogt@ipb-halle.de).

SUMMARY

Piperine (1-piperoyl piperidine) is responsible for the pungent perception of dried black pepper (*Piper nigrum*) fruits and essentially contributes to the aromatic properties of this spice in combination with a blend of terpenoids. The final step in piperine biosynthesis involves piperine synthase (PS), which catalyzes the reaction of piperoyl CoA and piperidine to the biologically active and pungent amide. Nevertheless, experimental data on the cellular localization of piperine and the complete biosynthetic pathway are missing. Not only co-localization of enzymes and products, but also potential transport of piperamides to the sink organs is a possible alternative. This work, which includes purification of the native enzyme, immunolocalization, laser microdissection, fluorescence microscopy, and electron microscopy combined with liquid chromatography electrospray ionization tandem mass spectrometry (LC-ESI-MS/MS), provides experimental evidence that piperine and PS are co-localized in specialized cells of the black pepper fruit perisperm. PS accumulates during early stages of fruit development and its level declines before the fruits are fully mature. The product piperine is co-localized to PS and can be monitored at the cellular level by its strong bluish fluorescence. Rising piperine levels during fruit maturation are consistent with the increasing numbers of fluorescent cells within the perisperm. Signal intensities of individual laser-dissected cells when monitored by LC-ESI-MS/MS indicate molar concentrations of this alkaloid. Significant levels of piperine and additional piperamides were also detected in cells distributed in the cortex of black pepper roots. In summary, the data provide comprehensive experimental evidence of and insights into cell-specific biosynthesis and storage of piperidine alkaloids, specific and characteristic for the Piperaceae. By a combination of fluorescence microscopy and LC-MS/MS analysis we localized the major piperidine alkaloids to specific cells of the fruit perisperm and the root cortex. Immunolocalization of native piperine and piperamide synthases shows that enzymes are co-localized with high concentrations of products in these idioblasts.

Keywords: *Piper nigrum*, piperine, specialized metabolism, alkaloid, enzyme purification, fluorescence microscopy, laser microdissection.

INTRODUCTION

Dried fruits of black pepper (*Piper nigrum*) are a popular spice since antiquity. The pungent perception of the peppercorns is due to the high concentrations of piperamides, specifically piperine (1-piperoyl piperidine), which binds to the transient receptor cation channel subfamily V member 1 (TRPV-1) causing the same pain perception as capsaicin, a structurally similar amide from *Capsicum* species (hot chili peppers) (Caterina et al., 1997). Despite its prominent use as a spice and many applications in traditional and modern medicine (Meghwal & Goswami, 2013), reports with respect to the *in planta* biosynthesis, storage, and biological function of piperine are rare. Already in 1987, Semler and Gross reported that piperine localization is not restricted to the fruits and minor amounts are present in all vegetative parts. Subsequently, they described a

piperine synthase (PS) activity from shoots of black pepper, rather than from fruits (Geisler & Gross, 1990). By a differential RNA sequencing (RNA-Seq) approach comparing various black pepper organs, we recently identified the transcripts encoding enzymes for three sequential piperine biosynthetic steps in black pepper fruits (Schnabel et al., 2020; Schnabel, Athmer, et al., 2021; Schnabel, Cotinguiba, et al., 2021). CYP719A37, a cytochrome P450 monooxygenase, catalyzes the formation of the 3,4-methylenedioxy group from feruperic acid to piperic acid, followed by an activating piperic acid CoA ligase and a terminal BAHD-type acyltransferase, termed PS, that catalyzes the amide bond formation between the piperoyl CoA-ester and the piperidine heterocycle towards piperine (Figure 1). Co-expression and high transcript levels of genes encoding all three enzymes favor the pathway to be preferentially present in immature fruits, consistent with storage of the final product piperine. This is in agreement with data provided by Fourier transform near infrared (FT-NIR) spectroscopy that detected piperine in the central fruit perisperm rather than the surrounding pericarp, although the resolution at the cellular level was not provided (Schulz et al., 2005). Nevertheless, minor transcript levels encoding these biosynthetic enzymes were also detected in other organs (Schnabel, Athmer, et al., 2021).

The PS acyltransferase in *P. nigrum* is part of a small gene family of similar BAHD-type acyltransferases that were identified in the black pepper genome (Hu et al., 2019). A second acyltransferase, termed piperamide synthase (PAS), with 63% identity at the amino acid level to PS, was also identified to be co-expressed in fruits with equally high transcript levels (Schnabel, Athmer, et al., 2021). In contrast to PS, PAS, at least *in vitro*, preferentially produces piperine isomers that are not detected in extracts of freshly harvested fruits, and therefore the role of PAS in the fruits remains obscure. Compared to PS, the enzyme displays a much higher substrate promiscuity *in vitro* (Schnabel, Athmer, et al., 2021).

So far, no information is available on the precise localization of piperine and the complete piperine biosynthetic pathway, specifically PS and PAS at the cellular or subcellular level. Likewise, it remains a mystery how the plant manages to store piperine in reportedly high concentrations of up to 9% in the fruits (Gorgani et al., 2017; Kato & Furlan, 2007) although the compound is poorly water-soluble. The original identification of a PS-like activity in black pepper shoots by Geisler and Gross (1990), irrespectively of the high transcript levels in fruits, indicated that enzyme activities might be separated from transcripts and products, which is the case for several alkaloids. In opium poppy (*Papaver somniferum*), transcripts encoding benzylisoquinoline alkaloids are localized in companion cells, whereas biosynthetic steps take place in neighboring sieve elements, from where the active compounds are translocated to laticifers (Beaudoin & Facchini, 2014). A complex scenario of biosynthesis and transport has been proposed for the terpene indole alkaloid vindoline, which accumulates in idioblasts of the leaf epidermis and is secreted via ATP-binding cassette transporters to the leaf surface, but also accumulates in laticifer cells during expansion of young leaves as determined by mass spectrometry (MS) imaging and single-cell metabolomics (Kulagina et al., 2022; Yamamoto et al., 2019; Yu & de Luca, 2014). Pyrrolizidine alkaloids are synthesized in specialized cells of the roots in *Senecio jacobea* and are translocated via the phloem to the sink organs, where they are further modified (Hartmann et al., 1989). In *Crotalaria* (Fabaceae), pyrrolizidine formation and transport is triggered upon nodulation with rhizobia in the roots from where the alkaloids are transported to the photosynthetic organs of the plant (Irmer et al., 2015). While also nicotine is translocated from the roots to the leaf vacuoles via the xylem, mediated by a MATE-type transporter (Morita et al., 2009), the pungent capsaicin in *Capsicum* species is stored and synthesized in interlocular septa of ripening fruits and apparently translocated into extracellular compartments termed blisters (Stewart et al., 2007). In some *Capsicum* varieties with a high capsaicinoid content, capsaicin can also be detected in neighboring fruit pericarp cells (Arce-Rodríguez & Ochoa-Alejo, 2019; Tanaka et al., 2021), presumably in vacuole-like structures (Fujiwake et al., 1980). Other natural products, specifically glucosinolates, are localized in millimolar concentrations in special idioblasts, where synthesizing and degrading enzymes are presumably separated in different compartments within the same cells (Koroleva et al., 2010).

Biosynthesis, transport, and storage of specialized metabolites is complex and far from being understood. In the case of piperine biosynthesis, investigation of the biosynthetic pathway is still at its infancy. Up to now, not

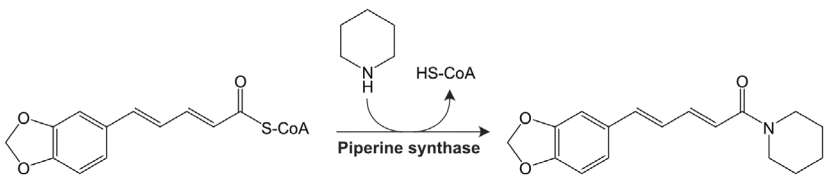

Figure 1. Piperine synthase catalyzes the formation of piperine from piperidine and piperoyl CoA.

even the final step catalyzed by PS joining substrates derived from two different biosynthetic routes, one presumably from phenylalanine and the other from lysine, has been established from intact plants or was localized to specific organs at the cellular level. In this report we used a combination of enzyme purification, immunolabeling, fluorescence and electron microscopy, laser microdissection, and liquid chromatography electrospray ionization tandem MS (LC-ESI-MS/MS) to provide several lines of evidence that in the case of piperine biosynthesis, enzymes, and products are co-localized in the same cells, presumably in specialized idioblasts of the fruit perisperm. Besides the fruit endosperm, piperine and piperamides are also present in cortex cells of the roots that may serve to store these alkaloids as an effective defense against biotic stressors (Scott et al., 2008).

RESULTS

Detection of PS in black pepper organs

Polyclonal antibodies were raised against purified recombinant PS and PAS and tested for their specificity against recombinant and plant enzymes. Antibodies detected the recombinant PS and PAS proteins with high sensitivity down to the nanogram range in Western blot analysis (Figure S1). However, the data also indicate that an immunological differentiation between recombinant PS and PAS was impossible with any of the four antibodies generated. A single antibody, termed PAS-AB1, specifically detected recombinant PS and PAS and also displayed fruit-specific signals of the appropriate size whereas the remaining antibodies cross-reacted with unknown proteins of higher molecular mass that were present in leaves and fruits (Figure S2). Since we never detected any trace of piperine in flowers and leaves, both organs served as negative controls to exclude any cross-reactivity, either caused by BAHD-type acyltransferases of different specificity (Hu et al., 2019) or by other unknown proteins. Therefore, PAS-AB1 was used subsequently to examine crude protein preparations of different black pepper organs for the presence of PS and PAS. Low-molecular-weight PS/PAS signals in the case of fruits observed in initial studies (Figure S2) are most likely degradation products and were eliminated by replacing the classic TCA-protein precipitation by a method published by Wessel and Flügge (1984) that gave suitable and reproducible results (Figure 2). Total protein extracts from different organs of black pepper as well as fruits at several developmental stages were prepared (Figure 2a,b) and tested for the presence of PS and PAS. A strong signal of the expected molecular mass is only observed in fruits at different developmental stages, whereas a signal for all other organs is not detectable at these protein concentrations (Figure 2a). During fruit development, the total levels of PS and PAS increase from 20 to 30 days post-anthesis (dpa) up to 75 dpa and decrease again over the next 3 months of fruit maturation until no distinct signal can be detected around 200–250 dpa in fully mature fruits that dropped off the spadix (Figure 2b). Only upon longer antibody and substrate exposure times with high protein loads a weak signal was detected in protein preparations from roots. Even then, no signal was ever observed in leaves or flowers. In summary, the Western blot results are consistent with rising piperine levels and the transcriptome data that suggest highest transcript abundance in fruits around 60 dpa (Schnabel, Athmer, et al., 2021). It is important to note that neither unspecific signals indicating no protein degradation in the optimized extraction protocol nor any cross-reactivity show up on any of the Western blots, consistent with an apparent high specificity of the purified polyclonal PAS-AB1

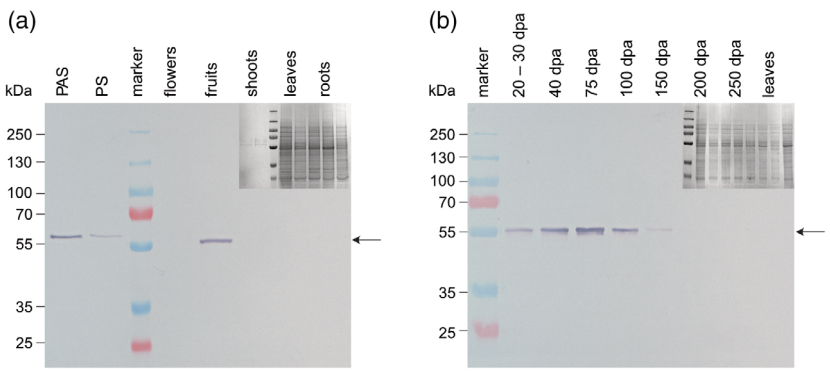

Figure 2. Detection of native PS and PAS.
(a) Organ-specific detection of PS and PAS. As a control, 10 ng of recombinant proteins was loaded.
(b) PS/PAS detection in *Piper nigrum* fruits at different developmental stages. Immunoblots were performed with anti-PAS-AB1 antibody at a dilution of 1:5000. As a secondary antibody, goat anti-rabbit IgG antibody conjugated to alkaline phosphatase was used at a dilution of 1:10 000. Development time was 5 min. No signals were obtained with the pre-immune serum. Signals of PS and PAS at 55 kDa are marked with an arrow. Each lane represents the total protein content of 10 mg of crude plant material. The corresponding SDS-PAGE gels are shown as small inserts in (a) and (b). PAS, piperamide synthase; PS, piperine synthase; SDS-PAGE, sodium dodecylsulfate–polyacrylamide gel electrophoresis.

antibody against PS/PAS. Yet, at this stage we were not convinced that PAS-AB1 indeed detected the correct native enzymes and unknown specificities could still interfere with the data.

Purification and annotation of PS and PAS from black pepper

In order to corroborate that native and enzymatically active enzymes are specifically detected by this antibody, we purified native PS/PAS synthase from immature fruits around 60–80 dpa, when highest activities were expected based on the transcript levels and immunoblot data. Before the present study, native PS/PAS enzymes and activities had never been purified. The initial PS-like enzyme activity obtained from shoot preparations was rapidly lost after a single ion-exchange purification step (Geisler & Gross, 1990). Excluding ion-exchange chromatography we purified PS/PAS activity by a combination of fractionated ammonium sulfate precipitation, hydrophobic interaction chromatography (HIC) on phenylsepharose, and subsequent size exclusion chromatography (SEC). High millimolar concentrations of ascorbic acid, included in the extraction buffer, were absolutely essential to prevent rapid oxidation and loss of enzyme activity. A strong signal of PS/PAS at 55 kDa that is observed by Western blot already in crude ammonium sulfate preparations (Figure 3) was enriched during HIC. After concentration and subsequent size fractionation, the highest PS/PAS enzyme activities eluted in SEC-fractions 10–14, which corresponded to a molecular mass of around 60 kDa, consistent with the molecular mass of a monomeric enzyme and the data from the recombinant PS/PAS, respectively (Schnabel, Athmer, et al., 2021). Up to now, it was not possible to separate native PS and PAS by any of the technologies used. This slightly higher than anticipated molecular mass of PS/PAS on sodium dodecylsulfate–polyacrylamide gel electrophoresis (SDS-PAGE) (approximately 55 kDa as compared to calculated 51 kDa) is in line with previous observations reported for other BAHD-type acyltransferases (D'Auria et al., 2002). Purified PS/PAS activities in all cases matched the signals on SDS-PAGE and immunoblots performed with the PAS-AB1 antibody. Again, a single band is detected in the crude protein preparation. Additional signal intensities of lower molecular mass during HIC and SEC purification steps therefore are enzyme degradation products. Signals of similar sizes were obtained during purification of recombinant PS and PAS from *Escherichia coli* and during initial extraction procedure of plant proteins (Schnabel, Athmer, et al., 2021; Figure S2).

To further confirm that isolated activities indeed represent PS and/or PAS and the PAS-AB1 antibody detects the correct signals in the immunoblots, the 55 kDa band of the SEC fraction (boxed in Figure 3) with the highest relative PS/PAS activity was extracted from the gel, digested with trypsin, and analyzed for PS/PAS peptide signatures (Table 1). Two independent experiments revealed a peptide coverage of 13% and 14% in the case of PS and a coverage of 23% and 26% in the case of PAS. No obvious post-translational modifications, e.g., phosphorylation or myristoylation, were observed in the peptide sequences obtained from both proteins. The data corroborate that the antibody detects the correct native PS and PAS proteins and transcript abundance is consistent with active protein production in immature black pepper fruits. In summary, as in the case of the recombinant enzymes, purification of native PS/PAS was successfully achieved and it was verified that both enzymes are present in immature fruits.

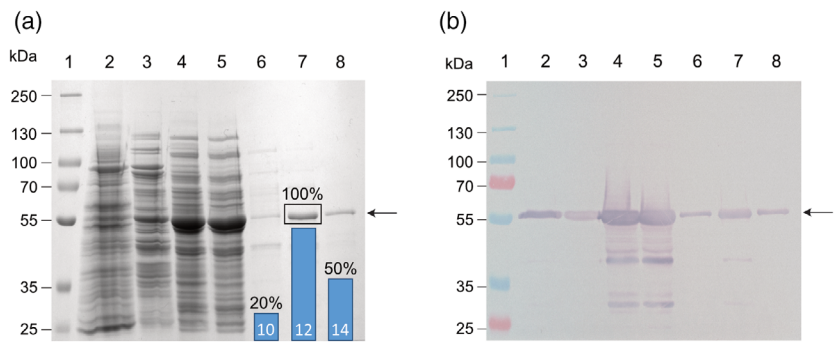

Figure 3. Purification of PS/PAS from black pepper fruits.
(a) Coomassie-stained 10% SDS-PAGE gels. SEC purification steps were analyzed and inserted blue bars represent relative PS/PAS activities. The highest activity in fraction 12 was set to 100%. 1, molecular size marker; 2, 30–85% ammonium sulfate fraction; 3, HIC fractions 2–32 with 10% of total activity; 4, HIC fractions 34–52 with 90% of total activity; 5, identical to 4, desalted and concentrated; 6, SEC fraction No. 10 (20% relative activity); 7, SEC fraction No. 12 (100% relative activity); 8, SEC fraction No. 14 (50% relative activity). The arrows mark the position of the PS/PAS activity and signal, respectively. The band representing the highest activity after SEC and sent for sequencing is boxed.
(b) Immunoblot illustrating the presence of the corresponding PS/PAS signals at 55 kDa. Antibody dilutions: first, 1:5000; second, 1:10 000. HIC, hydrophobic interaction chromatography; PAS, piperamide synthase; PS, piperine synthase; SDS-PAGE, sodium dodecylsulfate–polyacrylamide gel electrophoresis; SEC, size exclusion chromatography.

Table 1 Annotation of the most abundant peptides of purified PS and PAS obtained by digestion of the SDS-PAGE-extracted PS/PAS protein band and LC-ESI-MS/MS analysis

PS peptide	Amino acid sequence	PAS peptide	Amino acid sequence
PS 1	APSSQLEFNVVRK	**PAS 1**	LSDIDDQDGV
PS 2	ELSDIDDQDGLR	PAS 2	TDPASDIR
PS 3	AMVMYYPLAGR	PAS 3	AMVYYYPFAGR
PS 4	FAPDELSRLIIAVNAR	**PAS 4**	FACGGFIITGRFNHVMADAPGFTMFM
PS 5	VTEEYVK	**PAS 5**	AQLPADLR
PS 6	NGEEEGVVVPIRLPESAVGR	PAS 6	ATSFDIITACMWR
		PAS 7	VSALQYGPDEVVRLIVAVNSR
		PAS 8	LVGSDLGYAVELVR
		PAS 9	VTEEYVRSAADFLVLNGR

Peptide sequences were obtained from two individual experiments and matched. Average peptide coverage is 25% for PAS and 14% for PS. Bold letters denote that the peptide was present in both sequencing replicates.
LC-ESI-MS/MS, liquid chromatography electrospray ionization tandem mass spectrometry; PAS, piperamide synthase; PS, piperine synthase; SDS-PAGE, sodium dodecylsulfate–polyacrylamide gel electrophoresis.

Immunolocalization of PS and PAS in immature fruits

To localize PS and PAS at the cellular level, cross-sections of embedded immature black pepper fruits were monitored under a fluorescence microscope using PAS-AB1 and goat anti-IgG antibodies coupled to the fluorescent dye Alexa Fluor® 488. The corresponding images indicate that PS and PAS accumulate in special cells of the fruit perisperm (Figure 4a–f).

Fluorescing PS and PAS signals appear to be co-localized with residual cytoplasmic structures in these

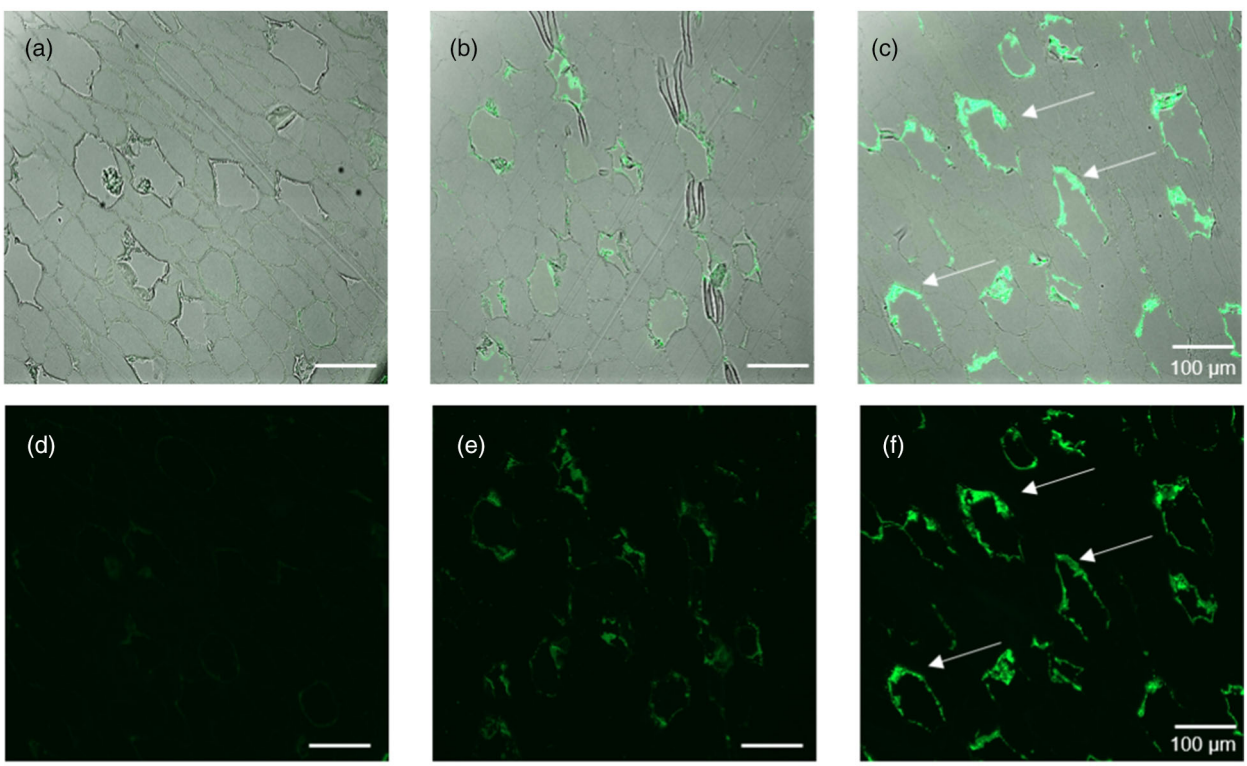

Figure 4. PS and PAS signals of black pepper cells of the fruit perisperm embedded in Technovit 7100. (a–c) Bright field and fluorescence overlay. (d–f) Only fluorescence signals. (a) and (d), without primary antibody; (b) and (e), pre-immune sera, secondary antibody coupled to Alexa Fluor® 488 (1:250); (c) and (f), PAS-AB1 antibody and secondary antibody coupled to Alexa Fluor® 488 (1:500), excitation at 493 nm and emission at 517 nm. Arrows mark the specific PS/PAS signals. PAS, piperamide synthase; PS, piperine synthase.

cells. Some signals were also observed when the pre-immune serum was used, but these signals are considerably weaker in all sections obtained. Some fluorescence signals were also observed from the cells surrounding the perisperm and also the pericarp (Figure S3). However, this fluorescence is already visible in the controls, when either no serum, i.e., only the secondary antibody, was used, or when the pre-immune sera were used in combination with the secondary antibody. These fluorescence signals may indicate unspecific cell wall autofluorescence and are most likely inconsistent with the presence of PS and PAS. Cells with the strongest fluorescence signals appear somewhat larger and at this mature stage already look slightly damaged. This was further examined by transmission electron microscopy (TEM) images of 40 dpa immature fruits that indicate some larger translucent perisperm cells of irregular shape among cells of 'normal' shape (Figure 5). These cells are not present in very early stages of development (6 dpa) when fruits start to develop and no piperine formation is detected (Schnabel, Athmer, et al., 2021). Details of these special cells are shown in Figure 5(f,g). The cells contain a cytoplasmic area; however, the only discernible organelles in the cytoplasm are proplastids and dictyosomes. A nucleus and mitochondria cannot be

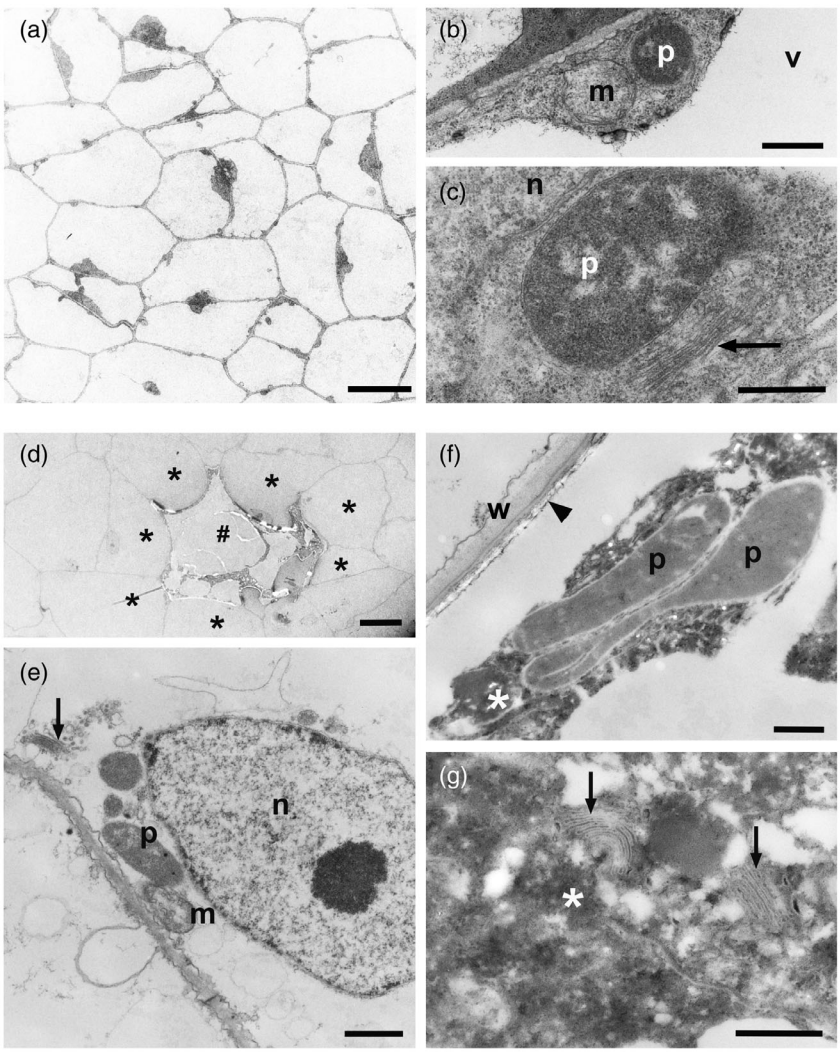

Figure 5. Ultrastructure of the perisperm. (a–c) At 6 dpa. (d–f) At 40 dpa. (a) Overview of the perisperm 6 dpa shows a single cell type containing a large vacuole and a thin layer of cytoplasm in the periphery of the cells. Scale bar, 10 μm. (b, c) Details of the cytoplasm. m, mitochondrion; p, plastid; arrow, dictyosome; v, parts of a vacuole; n, nucleus. Scale bars in (b, c) represent 0.5 μm. (d) Overview of two cell types in the perisperm 40 dpa. A single cell, morphologically similar to the labeled cells in Figure 4 (hashtag), is surrounded by 'normal' perispermal cells (asterisks). Scale bar, 10 μm. (e) Part of a 'normal' perispermal cell with nucleus (n), proplastids (p), mitochondrion (m), and a dictyosome (arrow). These cells omitting the tonoplast do not show the cytoplasmic matrix containing ribosomes. Scale bar, 1 μm. (f, g) Details of cells marked with a hashtag in (d). The cells contain a dense, dark cytoplasmic area (white asterisks) with proplastids (p) and dictyosomes (arrows). The cytoplasm seems to degenerate. The cell is not surrounded by a cell wall. There are only dark deposits (arrowhead) in the neighborhood of a cell wall (w) of a 'normal' perispermal cell. Scale bars in (f, g) represent 0.5 μm. dpa, days post-anthesis.

detected. The dark cytoplasm at this stage of development seems to degenerate. Surprisingly, the cell at this stage is not surrounded by a cell wall, and some dark deposits close to the cell wall of neighboring cells can be detected (Figure 5f). This special cell seems also partly detached from the neighboring cells (Figure 5d).

It was not possible to prepare material for TEM from fruits older than 40–50 dpa, due to the increasingly rigid structure of the perisperm that prevented efficient embedding in the epoxy resin. However, the TEM images of stages when piperine accumulation just started corroborate the presence of PS/PAS proteins in some specific cells that already underwent cellular reorganization and potential modification of organelles. This suggests transformation of cells into specific idioblasts suitable for piperine sequestration already at early stages of development. A comparable scenario of early cellular reorganization and subsequent apoptosis was observed in the case of *Brassica* idioblasts that accumulate high concentrations of glucosinolates and the corresponding biosynthetic enzymes (Koroleva et al., 2010).

Piperine localization and quantification in the fruit perisperm

Localization of piperine to the central perisperm of the peppercorn has been reported by FT-NIR spectroscopy however at a very moderate resolution (Schulz et al., 2005). The aromatic part of piperine in principle is a phenylpropanoid unit extended by an unsaturated C2 carbon unit and is responsible for the observed UV absorbance with a maximum at 345 nm. Somewhat dependent on the substitution pattern of the aromatic ring, phenylpropanoids also show a characteristic turquoise to bluish fluorescence when excited with short-wavelength UV light (Fraser & Chapple, 2011; Lang et al., 1991). The absorbance and fluorescence properties of piperine are known and have been listed in detail (Debnath & Mishra, 2020; Suresh et al., 2007). Therefore, we checked whether we could detect piperine by its autofluorescence. We examined cross-sections of black pepper fruits at different developmental stages for the presence of the expected cellular fluorescence. (Figure 6). A strong increase of turquoise signals inside the perisperm was observed from around 30 dpa to around 150 dpa (mature fruits) (Figure 6a). The blue fluorescence signals are concentrated in specific spots that likely represent individual cells. The distribution of these cells was comparable to the pattern observed in the PS/PAS immunolocalization study. None of these spots were detected in the surrounding pericarp.

In addition, we analyzed fresh fruit extracts by LC-ESI-MS including UV and fluorescence detection. The strong fluorescence signal with the same retention time as a piperine standard, corroborated by the expected UV signal at 345 nm and an *m/z* ratio of 286.1 $[M + H]^+$, confirmed

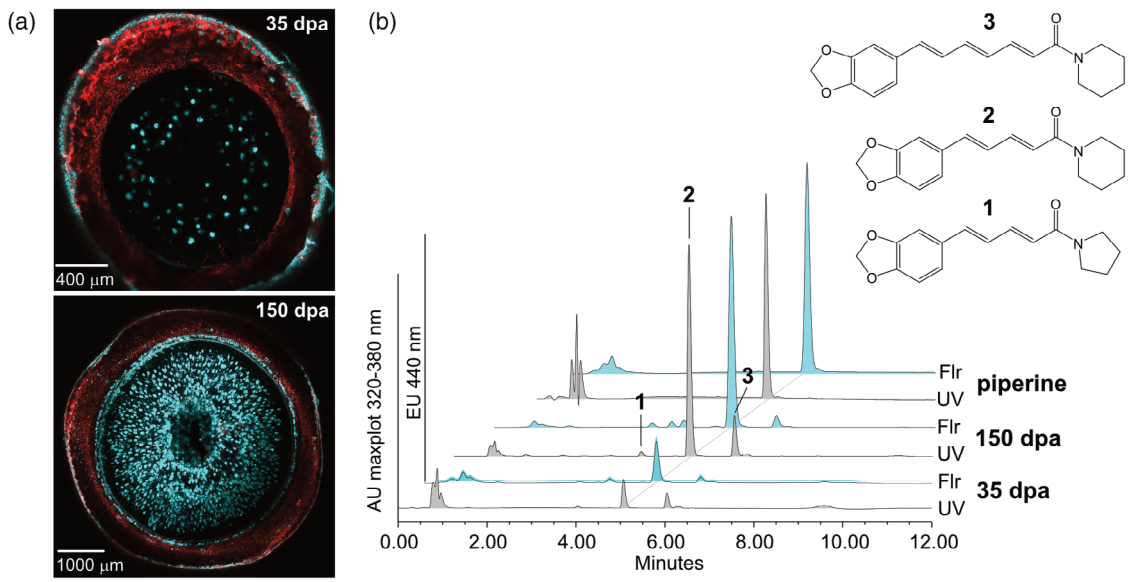

Figure 6. Fluorescence-based detection of piperine and piperamides in black pepper fruits.
(a) Cross-section of black pepper fruits at different developmental stages. Top, 30–40 dpa (mature); bottom, 150 dpa. The fluorescence excitation wavelength was 415 nm and emission was recorded at 474 nm.
(b) HPLC chromatograms from methanolic extracts of two corresponding developmental stages of fruit development (35 and 150 dpa), illustrating the strong increase in UV and fluorescence (Flr) signals for piperamides, specifically piperine, compared to a standard of 50 pmol piperine. UV signals at 320–380 nm with maxplot detection are shown in gray, fluorescence signals are shown in blue. The excitation wavelength was 350 nm and emission was recorded at 440 nm. Structures of piperoylpyrrolidine (1) *m/z* 272.1 $[M + H]^+$, piperine (2) *m/z* 286.1 $[M + H]^+$, and piperettine (3) *m/z* 312.1 $[M + H]^+$ are shown. Note that the signal intensity for the 35 dpa sample was upscaled 2-fold to be able to monitor the minor level of piperamides in comparison to the 150 dpa sample. dpa, days post-anthesis.

that mainly piperine is the source of this fluorescence (Figure 6b).

Two additional fluorescing piperamides were also identified in the extracts. Piperettine was described from black pepper fruits already in 1950 by Spring and Stark. Besides its fluorescence it is characterized by a bathochromic UV shift of 14 nm, 359 nm versus 345 nm in the case of piperine, and an *m/z* ratio of 312 $[M + H]^+$ consistent with an additional CH_2 group in the carbon chain. A minor fluorescence peak at *m/z* 272.1 $[M + H]^+$, N-piperoylpyrrolidine, was identified as the product of PS and PAS when piperidine was replaced by the heterocycle pyrrolidine (Schnabel, Athmer, et al., 2021). It displays a virtually identical fluorescence and UV spectrum as piperine. All three compounds account for the bluish fluorescence observed in cross-sections of the fruit pericarp. Piperine is the dominant alkamide in fruits, increasing more than 20-fold in mature fruits as compared to the fruits harvested at 20–40 dpa. This is consistent with the increasing numbers of bluish spots in the perisperm monitored under the microscope (Figure 6a). In fact, some of the fruits did not show any piperine signals at these early time points at all. Characteristic UV, mass, or fluorescence signals of additional phenylpropanoids like chlorogenic acid or caffeic acid derivatives were never detected in any LC-ESI-MS/MS screens. Blue spots observed in the pericarp represent polymeric cell wall material that is present throughout fruit development and is not extractable by methanol. LC-MS analysis indicated that minor amounts of non-fluorescing aliphatic amides are present in the fruits as reported previously (Chandra et al., 2004) that cannot be detected by fluorescence signals.

To further verify that the blue fluorescing spots in the fruits are the major source of the aromatic piperamides, individual cells were cut out by laser microdissection and extracted with 90% methanol. The data presented in Figure 7 show that only the fluorescing cells and not any of the surrounding, non-fluorescent tissue were the sole source of these compounds. Fluorescing fruit cells (Figure 7b) were extremely rich in piperine (Figure 7c) and accumulated to 2.0 ± 0.3 fmol μm^{-2} in contrast to neighboring cell with less than 10% of calculated amounts. The signal intensities of a single cell were sufficient to generate a strong peak in either UV-MS, or fluorescence-MS detection. In fact, the UV signal intensity represented by the chromatogram in Figure 7(d) corresponds to the methanol-extractable compounds of a single cell. To determine the piperamide, i.e., mostly piperine, concentrations in these

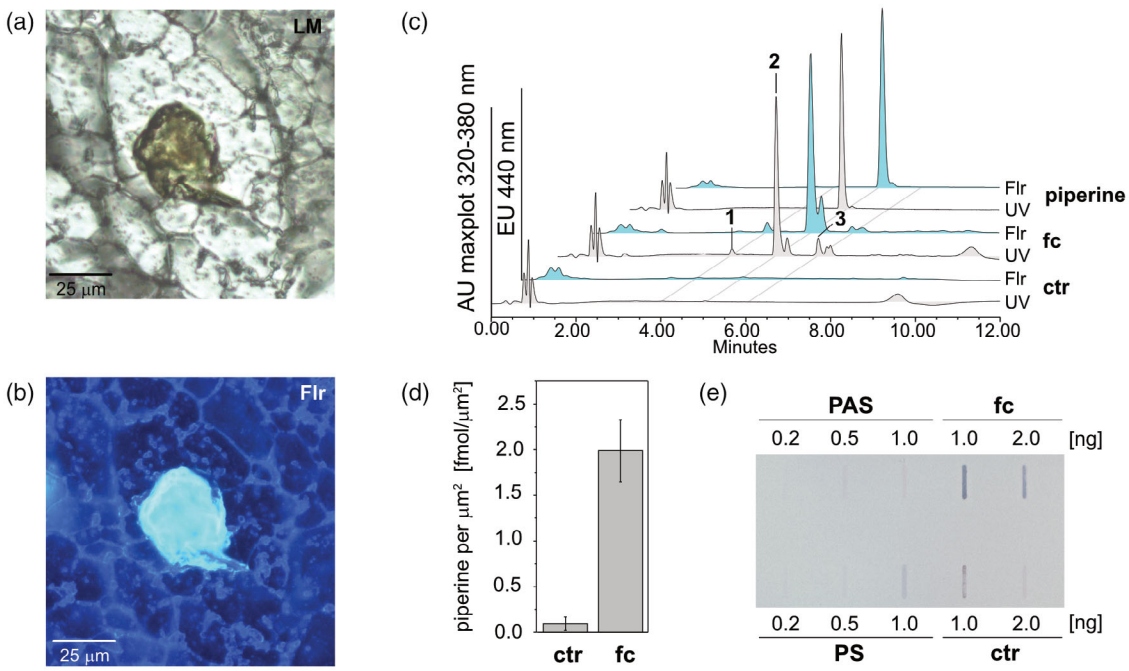

Figure 7. Laser microdissection of freeze-dried black pepper fruit cell layers (15 µm thickness). (a) Light microscopy image. (b) A corresponding blue fluorescing cell isolated from fruit. The excitation wavelength was 415 nm and emission was recorded at 474 nm. (c) LC-UV and LC-FLR detection of representative extracts of isolated surrounding control cells (ctr) and fluorescing cells (fc). Piperine standard, 50 pmol. UV absorbance at 320–380 nm with maxplot detection; fluorescence (FLR) was detected with excitation at 350 nm and emission was recorded at 440 nm. The signals shown in the chromatogram correspond to the piperine/piperamide content of a single cell. For identified compounds 1–3, piperoylpyrrolidine (*m/z* 272.1 $[M + H]^+$), piperine (*m/z* 286.1 $[M + H]^+$), and piperettine (*m/z* 312.1 $[M + H]^+$), see Figure 6. (d) UV-based quantitative analysis of fluorescence in fluorescing cells (fc) and surrounding control cells (ctr); ctr, 0.2 ± 0.2 fmol μm^{-2}; fc, 2.0 ± 0.3 fmol μm^{-2}. $n = 3$ (100 cells each). (e) Slot blot of protein extracts from isolated fluorescing fruit cells and neighboring cells using the anti-PS/PAS antibody and different concentrations of PS and PAS protein (0.2–1 ng) as a reference. Total protein extracts of (1.0) 600 cells and (2.0) 300 cells (fc or ctr) are blotted. PAS, piperamide synthase; PS, piperine synthase.

cells, the average volume comprising 100 cells was measured by an LSM 780 microscope based on the total area excised, multiplied by the thickness of the sections and divided by the number of cells. The resulting calculated volume of 0.007 μm^3 is equivalent to 7 nl per cell. The concentration of piperine on a per cell basis was subsequently calculated to an astonishing 4.30 $\pm$ 0.45 M based on a standard curve of piperine determined by UV absorbance at 345 nm.

In addition to the enzymatic products we were wondering if fluorescing and neighboring cells could be monitored for the presence of PS and PAS enzymes by immunoblotting. 300 and 600 cells, either blue fluorescing or non-fluorescing neighbor cells, were cut out, ultrasonicated, and immediately transferred to a slot blot in transfer buffer without SDS. Different concentrations of PS and PAS were applied as a reference signal (Figure 7e). We detected much stronger signals than we initially anticipated in the extracts of such a small number of cell material. We also detected some signals in neighboring non-fluorescing cells. Consistent with the data from the immunofluorescence measurements, we concluded that blue fluorescing parenchymatic cells of the fruits besides piperamides also harbor the enzymes that catalyze piperine/piperamide formation. Based on the weaker signals we observed in neighboring cells, we assumed PS and PAS biosynthetic enzymes were also present in these cells. This makes perfect sense, since the number of fluorescing spots increases during fruit maturation and it is very likely that these cells already contain PS, PAS, or both enzymes, subsequently accumulate piperamides at later stages of development, and develop into piperine storage cells.

Localization of piperamides in black pepper roots

We never detected any fluorescence signals of piperine or similar piperamides in leaves and flowers of black pepper. Browsing through the literature, it was puzzling that black pepper roots seemed to be investigated only once for piperamides and a complex pattern of some aromatic but mostly aliphatic compounds was reported (Wei et al., 2004). This is even more surprising since initial transcript data obtained from root tissue suggested that antimicrobial defense genes and compounds would be specifically expressed in the roots (Gordo et al., 2012). Based on minor transcript levels of PS and PAS detected in black pepper roots (Schnabel, Athmer, et al., 2021) we also tried to localize fluorescing piperamides in the roots. Methanolic root extracts contained three major fluorescing compounds (Figure 8). In contrast to the fruits, piperine was not the major aromatic piperamide. The dominant UV-absorbing compound peak with an *m/z* ratio of 260.1 $[M + H]^+$ was identified as methylenedioxycinnamoyl piperidine (ilepcimide). It shows a slightly reduced intense fluorescence compared to piperine that is likely caused by the fluorescence excitation signal that was optimized for piperine and is likely slightly different in the case of ilepcimide. Since a standard of this compound was not available, we synthesized ilepcimide by recombinant PAS that was able to catalyze the reaction of piperidine and methylenedioxycinnamoyl CoA that was produced as part

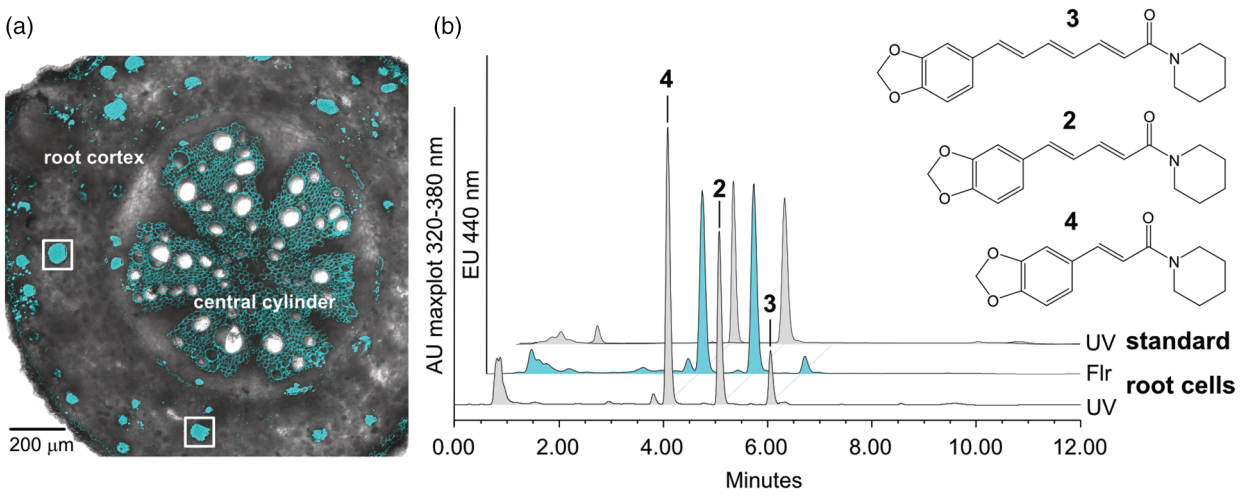

Figure 8. Cross-section through a root of black pepper.
(a) Fluorescing cortex cells that contain piperamides are marked.
(b) LC-UV (green) and corresponding LC-FLR (blue) signals of a root extract of black pepper. UV signals of a combined ilepcimide/piperine standard mix in grey. The structures of peak 4 (ilepcimide *m/z* 260.1 $[M + H]^+$), peak 2 (piperine), and peak 3 (piperettine) are shown. Compound 3 (piperettine) was verified based on retention time, UV absorbance (λ_{max}, 359 nm), its molecular mass (*m/z* 312.1 $[M + H]^+$), and its blue fluorescence. The blue fluorescence of the conductive tissue in the central cylinder in (a) was also analyzed and did not contain any soluble piperamides as determined by LC-ESI-MS, UV detection, and fluorescence detection.

of our previous investigations (Schnabel et al., 2020; Schnabel, Athmer, et al., 2021). The retention time, UV spectrum, and molecular mass of the enzymatically produced compound were identical with those of the compound detected in the roots. The molecular mass and spectroscopic data for the third, minor aromatic piperamide are consistent with those for piperettine, already identified from fruits. All structures identified from the roots are displayed in Figure 8(b). The total quantities of aromatic root piperamides were surprisingly high and amounted to 40% of the concentration of piperine on a per fresh weight basis.

When cross-sections of black pepper roots were analyzed by fluorescence microscopy we observed several blue fluorescing cells in the fruit cortex in addition to the fluorescing central cylinder (Figure 8a). These cortex cells in mature roots were less abundant compared to the fruits. Isolated fluorescent root cells also showed the dominant presence of ilepcimide (*m/z* 260.1 $[M + H]^+$) as compared to piperine and piperettine (Figure S4). The levels of piperine and piperettine however were reduced in these preparations as compared to ilepcimide. This is likely due to apparently non-quantitative extraction once the material has been transferred to the lids of the collection tubes specifically when very low amounts of amphiphilic or hydrophobic compounds are transferred, as in the case of piperamides (Goebel-Stengel et al., 2012). We were able to recover some remaining piperine and piperettine in repeated methanolic washes of the lid and tubes. Immunoblots performed with 300 cells did not give any signals with the anti-PS/PAS antibodies. This might be either due to a low overall protein abundance, due to protein degradation in the mature roots, as observed for fruits during maturation (Schnabel, Athmer, et al., 2021), or due to the fact that these compounds are synthesized by a different set of BAHD-like acyltransferases that do no cross-react with the PAS-AB1 antibody at low nanomolar concentrations.

DISCUSSION

The experimental data of this report shed light on the still enigmatic biosynthesis of piperamides in black pepper fruits and roots. BAHD-type acyltransferases that catalyze the decisive step in piperine and piperamide formation are co-localized with high concentrations of their product piperine in specific idioblasts of the fruit perisperm. A slightly different set of aromatic piperamides is present in presumably similar idioblasts of the root cortex.

Idioblasts in black pepper fruit perisperm develop into piperine production sites

Initiation of idioblast formation in the black pepper fruit perisperm at this point is unclear. TEM micrographs indicate that 3–4 weeks after anthesis, cells in the fruit endosperm appear different from the neighboring cells in terms of shape, size, and organelle content and follow the canonical model of developing idioblasts observed for several classes of secondary metabolites, like glucosinolates and alkaloids (Shirakawa et al., 2021; Uzaki et al., 2022). At the subcellular level, they differ with respect to the structure of the cytoplasm and the size and shapes of plastids. This switch from a normal cell to an idioblast spreads all over the perisperm and results in programmed massive production of piperine and related specialized metabolites during fruit ripening. As shown for the transcription profile of maturing fruits this transition goes along with in a massive increase of hundreds of transcripts of specialized metabolism, related not only to piperamide formation, but also to terpenoid and presumably flavonoid biosynthesis (Schnabel, Athmer, et al., 2021). The strong fluorescence and high abundance of piperamides facilitated the identification of the compounds in both organs, roots and shoots. At a certain point of development, the majority of the perisperm cells in the fruits appear to have completely switched to massive storage containers for piperine (Figure 6). Increasing piperine accumulation until around 3 months post-anthesis matches the increase in PS and PAS protein levels observed in our study (Figure 1). If the strong decline in enzyme levels observed during late stages of fruit development is the result of the massive piperine accumulation or simply the result of additional degenerative and proteolytic degradation cannot be answered at this stage. Master basic helix–loop–helix (bHLH) transcription factors like FAMA were shown to be responsible for the transition of meristematic cells into myrosin cells or guard cells in Brassicaceae (Shirakawa et al., 2021). A set of orthologous transcription factors might also trigger the transition to a piperine-producing cell in the black pepper perisperm. Yet, in our RNA-Seq dataset (Schnabel, Athmer, et al., 2021), no such fruit-specific bHLH candidates were co-expressed with transcripts related to piperine biosynthesis and specialized metabolism. The cellular localization of both PS and PAS in maturing fruits corroborates that transcript accumulation matches the production of enzymes, i.e., PS and PAS, in black pepper fruit idioblasts. Previous investigations have shown that PS is quite specific for piperoyl CoA, while PAS is not. This raised doubts if this enzyme is actually present in the fruits. Purification of PS and PAS and identification of peptide PAS fragments unequivocally demonstrate that both acyltransferases are present. The substrate promiscuity of PAS, which does not fit with its substrate specificity for piperine *in vitro* combined with a reported diverse array of aliphatic and aromatic piperamides including piperettine in the fruits (Chandra et al., 2004), now asks for alternative PAS substrates that remain to be identified. The CoA-ester of piperettic acid, which is not commercially available, might be one candidate. However, it is also possible that *in vivo* the correct

isomers of piperine are synthesized by PAS. Channeling of metabolites in a presumed metabolon may influence enzyme specificity (Laursen et al., 2016; Møller & Conn, 1980). Under low amine and CoA-ester concentrations *in vivo* even the specific PS hydrolyzes piperoyl CoA to piperic acid and produces considerable amounts of piperine isomers, not detected in fruit extracts of black pepper.

Two scenarios for storage of piperine at the site of biosynthesis in high concentrations

Co-localization of enzymes and metabolites in the same cells eliminates the requirements for a plethora of still poorly understood regulatory and transport logistics reported for benzylisoquinoline or terpene indole alkaloid production (Dastmalchi et al., 2019; St-Pierre et al., 1999; Yamamoto et al., 2019). Even in the most extensively analyzed pathway of benzylisoquinoline alkaloid biosynthesis numerous questions on translocation between different cell types remain and favor an apoplastic transport between sieve elements, companion cells, and laticifers, summarized in Ozber and Facchini (2022). The on-site deposition of products within the biosynthetic cells provides a much simpler scenario and may also enable the plant to store the compounds in the extremely high amounts observed as in the case of black pepper fruits. Based on UV absorbance measurements, single cells of the fruits store the dominant compound, piperine, in molar concentrations. The concentration of total piperamides in the root idioblasts appears to be in the same order of magnitude. On a larger scale, this is equivalent to more than 1 kg alkaloid L^{-1}, and this is incomprehensibly high considering that piperine and other piperamides are poorly soluble in water with a lipid/water partition coefficient of 179.33 determined for piperine (Gorgani et al., 2017). In addition, piperine rapidly isomerizes in aqueous solutions which is apparently not the case in intact fruits. How can piperamides be synthesized and stored in these cells at such high concentrations without isomerization? One solution might come from the liverwort *Marchantia polymorpha*, where oil bodies surrounded by a single membrane not only store isoprenoids but also harbor some of the biosynthetic enzymes of terpene biosynthesis (Suire et al., 2000). The authors postulate a dynamic role of these oil bodies to accumulate and sequester lipophilic metabolites. Fluorescing droplets that apparently harbor piperamides may indicate that this process is also active in black pepper and may result in the extremely high concentrations observed. The perisperm essentially develops into a seed, a reproductive unit that germinates upon removal or digestion by bats and birds that consume the energy-rich pericarp of black pepper and secrete the perisperm with an embryo virtually undigested and therefore are effective dispersers of different *Piper* species (Baldwin & Whitehead, 2015). In black pepper, piperamides therefore are probably stored in oily droplets with a total of more than 50 different lipids and terpenoids reported from the oleoresin of black pepper fruits (Kapoor et al., 2009). Local, massive concentrations of phenylpropanoid-derived compounds are proposed for vacuolar anthocyanins, and reported also for 4-*O*-(3-methoxybenzaldehyde)-β-D-glucoside (vanilloyl glucoside) from *Vanilla planifolia* (Brillouet et al., 2014). Vanilloyl glucoside does not accumulate in vacuoles like glycosylated anthocyanidins or flavonoid glycosides, but is stored in redifferentiated chloroplasts, termed phenyloplasts, apparently in amorphous deposits. Concentrations of this glycoside on a per cell basis are comparable to piperine levels detected in our study. Like in the case of piperamides, the compound is also co-localized with a degrading enzyme, presumably a β-glycosidase, in the same cells but a different compartment that hydrolyzes the compound to vanillin and glucose upon cell rupture or degradation during fruit ripening. Within the cells, alkaloids like berberine in *Coptis japonica* or nicotine in *Nicotiana tabacum* roots are translocated to the vacuole for storage by proton-dependent ATP-binding cassette or purine uptake permease-like (PUP) transporters (Jelesko, 2012; Otani et al., 2005). Currently, we cannot comment if any active transport to specific compartments is involved in early phases of piperine translocation. Specific transporters that are co-expressed with any of the piperine biosynthesis genes do not show up in the RNA-Seq dataset (Schnabel, Athmer, et al., 2021). During late stages of cell maturation TEM pictures of presumably piperine-accumulating cells seem to indicate that these cells degenerate, tonoplasts and cell walls are non-existent, and therefore active transport to a specific organelle appears unlikely.

While accumulation in a lipophilic sphere is one option, storage in natural deep eutectic solvents (NADESs) provides an interesting alternative (Choi et al., 2011; Knudsen et al., 2018). Water-insoluble compounds like cannabinoids can be stored at high concentrations in specific compartments within a mixture of sugars, proline, amines, and organic acids while enzyme activities can also be conserved, even if water is largely or completely excluded (Knudsen et al., 2020; Rodziewicz et al., 2019). This may also explain why a single piperine isomer is detected and stabilized in dried black peppercorns presumably by hydrogen bond interactions (Dai et al., 2014), whereas in aqueous, methanolic solutions rapid isomerization occurs. In a report by Pavoković et al. (2020), enantioselective reduction of an aromatic ketone to an alcohol was reported when a plant cell culture was used with NADES as a green catalyst. The water content of the NADES solution also determined the enantiomeric ratio of the resultant alcohols. These solutions may not only explain the preference for a single piperine isomer, but could also provide a possible explanation for the different isomers generated by PAS *in vitro* and *in vivo*.

While storage of piperine in idioblasts at these high concentrations raises one question, potential remobilization and recycling of the stored nitrogen described for other nitrogen-containing metabolites like cyanogenic glucosides is another (Pičmanová et al., 2015). Piperine levels drop slightly during late fruit development (Schnabel, Athmer, et al., 2021), but the young seedling during germination is virtually devoid of any piperine. More than 95% of piperine remains in the dried seed shell (Figure S5). While we cannot exclude that some piperine is recycled as a nitrogen source for the developing embryo, we have never detected any piperine degradation products, specifically the free piperic acid or related phenylpropanoids, at any stage of fruit development, making recycling of a larger portion of piperine quite unlikely.

Piperamides in root idioblasts may serve as a defense against root pathogens

Piperamide-containing cells with similar fluorescing properties and composition are not only present in fruits but also in the root cortex. It is peculiar that in these cells, ilepcimide, not detected in the fruits, is the dominant compound rather than piperine and piperettine. Ilepcimide with an aromatic methylenedioxy group can be synthesized from ferulic acid derived from the classical phenylpropanoid pathway and does not require chain elongation compared to piperine or piperettine. It is likely that a different blend of enzymes is responsible for root piperamide formation already starting with a CoA ligase of different specificity than the specific piperoyl CoA ligase reported (Schnabel et al., 2020). Enzymatic and molecular investigation of black pepper roots has just started by us and others. A CoA ligase with a specificity for 3,4-methylenedioxycinnamic acid resulting in the CoA-ester has been characterized for black pepper (Jin et al., 2020) and is a good candidate within the biosynthesis of ilepcimide. Using the set of antibodies it was surprising that we could not detect PS and PAS in the roots. It is plausible that among the various BAHD-type acyltransferase genes identified in the genome (Hu et al., 2019) either enzymes with an altered specificity and sequence identity are present in the roots, or the total amount of biosynthetically active enzymes is strongly reduced compared to the fruits that show a clear development within a few months. The altered blend of compounds in the root idioblasts as compared to the fruits may represent an adaptive and more effective defense mechanism against specific root pathogens. From numerous investigations it is known that piperamides have a wide array of antimicrobial and insecticidal properties (Scott et al., 2008). Hao et al. (2016) in their analysis of the resistant *Piper flaviforum* versus susceptible *P. nigrum* noticed a stronger increase of phenylpropanoid-related transcripts in the resistant ones after infection with *Phytophthora capsici*, specifically genes encoding enzymes of the core phenylpropanoid pathway, phenylalanine ammonia lyase (PAL), 4-coumaroyl CoA ligase (4-CL), cinnamoyl CoA reductase (CCR), and cinnamoyl alcohol dehydrogenase (CAD). Moreira et al. (2017), analyzing the black pepper root transcriptome upon infection with *Fusarium solani* f. sp. *piperis*, also detected significant and strong responses of transcripts related to the mevalonate (MVA) and methylerythritol 4-phosphate (MEP) pathways, specifically genes encoding 3-hydroxy-3-methylglutaryl CoA reductase (*HMGR*) and 1-deoxy-d-xylulose-5-phosphate synthase (*DXS*). They did not report on any aspects of the piperamide metabolism likely due to the lack of orthologs in the Arabidopsis genome their comparison was based on. Otherwise piperamides in roots might accumulate over a much longer period of time, while the transcripts are not induced or are of lower abundance. Root idioblasts represent only a very small fraction of the root cortex and central cylinder compared to their high abundance in maturing fruits. The essential oil of *Piper marginatum* roots also contains a plethora of mono-, sesqui-, and diterpenoids (Bay-Hurtado et al., 2016) that have not yet been analyzed in black pepper roots. The blend of piperamides identified in the roots of black pepper may act synergistically with terpenoids that are likely produced, e.g., during *F. solani* f. sp. *piperis* infection as a highly effective underground defense cocktail against microbes and herbivores (Dyer et al., 2003). Fluorescence-guided laser microdissection combined with single-cell metabolomics and transcriptomics should allow to unravel the complete blend of compounds within these specialized fruit and root idioblasts in different Piperaceae and simultaneously shed some light on the factors required for storage of these compounds within the cells.

Taken together, by the functional characterization and localization of PS and PAS, we have just started to understand the multiple facets of piperine and piperamide biosynthesis in the perisperm of the fruits and the root cortex of black pepper. Several biosynthetic steps that comprise chain elongation of the presumed precursor feruloyl CoA as well as piperidine formation still require molecular and enzymatic evidence. Analytical and molecular tools to characterize cell-specific aspects of piperine biosynthesis, including MS imaging of potential precursors and single-cell RNA-Seq, are available to corroborate the cellular localization of the pathway within specialized cells of the ripening fruit endosperm. This will depend on careful experimental adjustments to a non-model species highly recalcitrant to engineering and transformation.

EXPERIMENTAL PROCEDURES

Plant material and chemicals

Cuttings from black pepper (*P. nigrum* L.) plants were originally obtained from the Botanical Garden of the University of Vienna

(Austria), from plants collected in 1992 (IPN No. LK-0-WU-0014181). Black pepper plants were grown under controlled greenhouse conditions at 24°C (day) and 18°C (night) with supplemental illumination for 14 h. Total irradiance was recorded at approximately 150 μmol m^{-2} sec^{-1}, including supplemental illumination. Plants were grown until fruits reached full maturity. For protein preparation and Western blot analysis, fruits and roots at different developmental stages, leaves, and flowers were frozen in liquid nitrogen and crushed to a fine powder using a mortar or a ball mill (Retsch, Haan, Germany). If the material was not processed directly, it was stored at −80°C. All chemicals including buffers, solvents, and standards, like piperine, were obtained from Merck (Darmstadt, Germany), Carl Roth (Karlsruhe Germany), Serva (Heidelberg, Germany), Thermo Fisher Scientific (Dreieich, Germany), or as indicated.

Antibodies and immunolocalization

Polyclonal antibodies were raised against recombinant PS and PAS (Schnabel, Athmer, et al., 2021) in two white New Zealand rabbits each. One milligram of purified proteins was injected in subsequent immunizations according to standard protocols by the manufacturer (Proteogenix, Schiltigheim, France). Sera of polyclonal antibodies were purified on Protein A Agarose (Thermo Fisher Scientific) according to the protocol supplied by the manufacturer. Briefly the crude sera were applied to the resin in neutral potassium phosphate (pH 7.5), unbound proteins were washed off, and purified antibodies were eluted with 100 mM glycine adjusted to pH 3.0. One third volume of 1 M Tris/HCl (pH 8) solution was added to each fraction immediately to adjust the final pH to neutral. The purified antisera were stable at 4°C for several days and aliquots were frozen at −80°C. Goat anti-rabbit IgG (Merck) for Western blot analysis at concentrations of 1:5000 or 1:10 000 and goat anti-rabbit IgG conjugated to Alexa Fluor® 488 (Thermo Fisher Scientific) at a concentration of 1:500 for immunolocalization were used.

Protein preparation and Western blot

Crude protein extracts from plant material were prepared according to a protocol developed by Wessel and Flügge (1984) with slight modifications. Fifty milligrams of ground plant material was dissolved in 1 ml extraction buffer (1 M Tris/HCl, pH 8.0, combined with 0.1 M sodium borate, pH 7.5, [36:44]; 1% insoluble Polyclar AT; 50 mM ascorbic acid; 10 μl plant protease inhibitor cocktail per ml buffer, and 5 mM 2-mercaptoethanol), ultrasonicated for 5 min, centrifuged for 10 min at 20 000 ***g***, and place on ice. Next, 200 μl of the supernatant was mixed with 800 μl of MeOH and 200 μl chloroform and samples were vortexed vigorously. Next, 600 μl of H_2O was added, and the solutions were vortexed and centrifuged for 15 min at 15 000 ***g***. The upper phase was carefully removed, 600 μl MeOH was added to the rest, and samples were vigorously mixed and centrifuged. The supernatant was discarded, and the protein pellets were dried at room temperature, dissolved into 100 μl resuspension buffer (100 mM Tris/HCl, pH 8.0), combined with an equal volume of SDS loading buffer, and heated to 95°C for 5 min. For Western blot analysis, equal amounts of total crude protein were loaded per lane (tested initially with a defined set of loading volumes). In the case of purified PS and PAS, concentrations were determined based on calculated extinction coefficients of recombinant enzymes, resulting in concentrations of 0.9 mg ml^{-1} PS and 1.04 mg ml^{-1} PAS to give an absorbance of 1.0 at 280 nm (Protean, Lasergene Software package; DNAStar, Madison, WI, USA). A PageRuler™ Plus Prestained Protein Ladder (Thermo Fisher Scientific) was used as a size marker. Proteins were separated by 10% SDS-PAGE and stained with Coomassie Brilliant Blue or used for Western blot analysis.

For Western blot analysis, proteins were transferred to 0.2 μm Protran Premium nitrocellulose membranes (GE Healthcare, Chicago, IL, USA) with a slightly alkaline transfer buffer according to the manufacturer. The membranes were pre-incubated with blocking buffer (5% non-fat dry milk) overnight, incubated with primary antibody (1:5000) for 2 h, washed with transfer buffer, incubated with secondary antibody coupled to alkaline phosphatase (1:10 000) in non-fat dry milk for 1 h, and rewashed in transfer buffer. Signals were developed using a colorimetric assay with 115 mM 5-bromo-4-chloro-3-indoxyl phosphate/61 mM nitroblue tetrazolium in dimethylformamide (DMF) according to standard protocols. The reaction was stopped with water after 1–20 min depending on signal intensity.

Immunolocalization and laser microdissection

For immunolabeling, fresh black pepper fruits harvested between 50 and 80 dpa were quartered using a razor blade, fixed for 2 × 2 h in 4% paraformaldehyde (PFA), washed in PBS, and dehydrated in a series of increasing ethanol concentrations from 10 to 100% at room temperature over 24 h. Subsequently, all steps were performed at 4°C. The ethanol solution was removed and the material was transferred to a series of increasing infiltration solutions (100 ml Technovit 7100 and 1 g hardener 1 [Kulzer, Werheim, Germany]) and 2 ml PEG 400 in ethanol in ratios of 1:3 for 4 h, 1:1 overnight, and 3:1 for 8 h and solidified by incubation in pure infiltration solution for 12 and 8 h, respectively. Finally the samples were placed in embedding solution (infiltration solution with 5% hardener, v/v), sealed with Aclar foil (Ted Pela, Redding, CA, USA), left overnight at 4°C, and cleaned with ethanol. Next, 2-μm sections were cut using a motorized microtome HM355 (Thermo Fisher Scientific), transferred to water drops on 'superfrost' slides (Thermo Fisher Scientific) to stretch them evenly, and incubated on a heating surface of 40°C to fix samples overnight.

For immunolabeling, sections were washed with PBS and subsequently incubated in 5% ammonium chloride to block aldehyde groups. Sections were washed again with PBS and incubated with 5% BSA (w/v) for 30 min. Subsequently primary antibodies or pre-immune sera were added to final ratios of 1:500 and 1:250, respectively, and samples were incubated at 4°C overnight. Samples were washed with 0.1% BSA (w/v) and subsequently 1% BSA (w/v) for 10 min each. The secondary antibody, anti-rabbit IgG conjugated to Alexa Fluor® 488 (Thermo Fisher Scientific), in 5% BSA (w/v) was added in ratios of 1:500 or 1:250 in the case of the pre-immune sera and samples were incubated at 37°C for 90 min in the dark to preserve the signal of the fluorophore. Slides were washed once with PBS, incubated with 4′,6-diamino-2-phenylindole, and washed again with PBS, and finally cover slips were mounted using ROTI® Mount FluorCare. Slides were stored in the dark until analysis. The Alexa fluorophore was excited at 493 nm, and emission was recorded at 513 nm using an Axio Imager Z2 (MembraneSlide 1.0 PEN; Carl Zeiss, Jena, Germany) with an Axiocam 506 objective Plan-Apochromat 20×/0.75 with the following settings: filter set excitation, BP 450–490; beam split, 510 nm; emission, LP 515.

For laser microdissection fresh samples were placed in small metal boats placed on dry ice. Water was added to the samples until fully submerged. The samples were carefully frozen for 15 min, kept at −20°C overnight, cut into 15-μm sections using a cryomicrotome Leica CM1950, placed onto coated slides (MembraneSlide 1.0 PEN; Carl Zeiss), and freeze-dried overnight. Between 100 and 1000 cells were cut out and shot into 200-μl tubes with adhesive caps (Carl Zeiss) using a laser Palm

Microbeam (Carl Zeiss). Piperine detection via fluorescence was achieved using hand-cut cross-sections of freshly harvested fruits and roots incubated in 10 mM aqueous ascorbic acid solution to prevent oxidation, and images were analyzed using an LSM780 fluorescence microscope equipped with Plan Neofluor 10×/0.3 (Carl Zeiss) at an excitation wavelength of 405 nm and emission at 415–474 nm and at 662–735 nm to monitor chlorophyll fluorescence simultaneously.

Transmission electron microscopy

For electron microscopy young immature black pepper fruits (15 and 40 dpa) were fixed with 3% glutaraldehyde (Merck) in 0.1 M sodium cacodylate buffer (pH 7.2) sodium cacodylate buffer (SCB) for 4 h, subsequently washed in SCB, post-fixed for 1 h with 1% osmium tetroxide (Carl Roth) in SCB, dehydrated in a graded series of ethanol, and finally embedded in epoxy resin (Spurr, 1969). Ultrathin sections (80 nm) were analyzed with an EM 900 (Zeiss) transmission electron microscope (acceleration voltage 80 kV). Electron micrographs were taken with a slow scan camera (Variospeed SSCCD, SM-1 k-120; TRS, Moorenweis, Germany).

LC-ESI-MS analysis of piperine and piperamides

For LC-ESI-MS analysis freshly harvested organs were frozen in liquid nitrogen, crushed to a fine powder using a ball mill (Retsch, Haan, Germany), dissolved at a concentration of 10 mg ml^{-1} in 90% methanol, ultrasonicated for 5 min, and centrifuged for 10 min at 21 000 ***g***, and the supernatant was transferred to dark tubes to prevent isomerization. Crude samples were diluted to a final concentration of 1 mg ml^{-1} in 90% MeOH and analyzed for piperine content and related amides using a Waters Alliance 2690 HPLC coupled to 2996 photodiode array, 2475 fluorescence, and QDA single quadrupole mass detectors (Waters, Eschborn, Germany). Either 100 (roots) or 100–300 (fruits) cells were prepared by laser microdissection, dissolved in 100 µl of 90% MeOH, briefly ultrasonicated, and centrifuged for 5 min at 20 000 ***g***. The supernatant was diluted up to 5-fold, and an aliquot was subsequently analyzed by LC-MS/MS. For LC-based analysis, a C_{18} reverse phase Nucleoshell 50/4 column (Machery-Nagel, Düren, Germany) with a solvent gradient from 30 to 80% acetonitrile (solvent B) in 0.1% aqueous formic acid (solvent A) within 7 min was used. Piperine concentrations were calculated based on a piperine standard (Carl Roth) in 90% methanol with UV detection at 345 nm or between 320 and 380 nm from 10 to 500 pmol per injection. Simultaneous detection of piperine (*m/z* 286.1 $[M + H]^+$) was performed by ESI with the QDA detector in positive ionization mode at a cone voltage of 15 V. Fluorescence signals of piperine and piperamide were recorded using an excitation wavelength of 350 nm and an emission wavelength of 440 nm.

Partial purification of PS from black pepper fruits

PS was purified from 50 g immature black pepper fruits (40–100 dpa) extending the original protocol by Geisler and Gross (1990) by a series of modifications. Frozen, crushed fruits were suspended in 250 ml of 1 M Tris/HCl and 0.1 M sodium borate (pH 7.5) (36:44) with 6% Polyclar AT (Serva), 50 mM ascorbic acid, 10 mM β-mercaptoethanol, and 3 µl protease inhibitor cocktail per ml extract (Merck). The suspension was stirred for 20 min on ice and centrifuged for 10 min at 20 000 ***g*** at 4°C, and the supernatant was filtered through two layers of Miracloth (Merck), mixed with a combination of 0.05% protamine sulfate (w/v) and 30% ammonium sulfate (w/v), stirred for 15 min, centrifuged for 10 min at 20 000 ***g***, and refiltered through Miracloth. Ammonium sulfate was added slowly to the filtrate to a final concentration of 80% (w/v), and samples were stirred for 30 min at 4°C and centrifuged for 20 min at 20 000 ***g***. The protein pellet was diluted in 1 M ammonium sulfate, 50 mM Tris/HCl (pH 7.5), 5% glycerol, and 5 mM DTT and fractionated on 20 ml phenyl sepharose filled into an XK16/20 column (Cytiva, Freiburg, Germany) by decreasing the ammonium sulfate concentration at a flow rate of 1 ml min^{-1}. Active fractions were pooled, concentrated on Centricon 10 membranes (Merck), and loaded onto a Superdex 200 Increase SEC 30/100 column (Cytiva) equilibrated in SEC buffer (50 mM Tris/HCl, pH 7.5, 150 mM NaCl, 5% glycerol, 5 mM DTT). SEC was performed at a flow rate of 200 µl min^{-1} on an Äkta Explorer FPLC (Cytiva) equipped with UNICORN 5.2 software. Finally, 500-µl fractions were tested for enzyme activity as described previously (Schnabel, Athmer, et al., 2021), concentrated, separated by SDS-PAGE, and subjected to peptide sequencing and identification.

Protein digestion and LC-MS/MS based analysis

SDS-PAGE-separated proteins were in-gel digested with trypsin and desalted as described by Majovsky et al. (2014). Dried peptides were dissolved in 5% acetonitrile with 0.1% trifluoroacetic acid and injected into an EASY-nLC 1000 LC system (Thermo Fisher Scientific). Peptides were separated using LC C_{18} reverse phase chemistry, employing a 120-min solvent gradient increasing from 5 to 40% aqueos acetonitrile in 0.1% formic acid at a flow rate of 250 nl min^{-1}. Eluted peptides were electrosprayed on-line into a QExactive Plus mass spectrometer (Thermo Fisher Scientific). The spray voltage was 1.9 kV, the capillary temperature was 275°C, and the Z-Lens voltage was 240 V. A full MS survey scan was carried out with the chromatographic peak width set to 15 sec, a resolution of 70 000, an automatic gain control (AGC) of 3×10^6, and a max injection time of 100 msec. MS/MS peptide sequencing was performed using a Top10 DDA scan strategy with HCD fragmentation. MS/MS scans with *m/z* ratios between 400 and 1850 were acquired. MS/MS scans were acquired with a resolution of 17 500, an AGC of 5×10^4, an injection time of 50 msec, an isolation width of 1.6 *m/z*, and a normalized collision energy of 28 eV, under a fill ratio of 3%, a dynamic exclusion duration of 20 sec, and an intensity threshold of 3×10^4.

Peptides and proteins were identified using Mascot software v2.7.0 (Matrix Science) linked to Proteome Discoverer v2.1 (Thermo Fisher Scientific). A precursor ion mass error of 10 ppm and a fragment ion mass error of 0.02 Da were tolerated in searches of the *Arabidopsis thaliana* TAIR10 database amended with pepper target proteins and common contaminants. Carbamidomethylation of cysteine (C) was set as fixed modification and oxidation of methionine (M) was tolerated as a variable modification. A peptide spectrum match (PSM), peptide, and protein level false discovery rate was generated for all annotated PSMs, peptide groups, and proteins based on the target decoy database model and the Target Decoy PSM Validator module. PSMs, peptide groups, and proteins with q-values beneath the significance threshold $\alpha = 0.01$ for PSMs and peptide groups and $\alpha = 0.05$ for proteins were considered identified.

DATA HANDLING AND DEPOSITION

All data will be deposited in the publicly available database RADAR (www.radar-service.eu) and accessible by the following DOI number: https://doi.org/10.22000/607. Raw data of the HPLC runs and images were also stored and secured on local IPB servers and hard drives and are available from the corresponding author (TV) upon request. Imaging, laser dissection, and all HPLC runs have been performed at least

three times from independent experiments. LC-MS/MS analyses of PS/PAS peptides have been performed from two independent SEC runs from HIC-purified proteins.

ACKNOWLEDGMENTS

We thank Simone Fraas (Electron Microscopy Lab, Martin-Luther-University Halle-Wittenberg) for her help in preparing the fruits for TEM. We thank Jörg Ziegler (IPB, Halle) for critical reading of the manuscript. Generous financial support of this project by the Deutsche Forschungsgemeinschaft (DFG, VO 719 15-1/2) is gratefully acknowledged. Open Access funding enabled and organized by Projekt DEAL.

AUTHOR CONTRIBUTIONS

LJ and AS performed experiments and analyzed data, HS analyzed data and provided experimental advice, UK performed experiments, SM and GH performed experiments and analyzed data, and TV designed research, analyzed data, and wrote the manuscript with support from all co-authors. The final version was approved by all authors.

CONFLICT OF INTEREST

The authors have not declared a conflict of interest.

SUPPORTING INFORMATION

Additional Supporting Information may be found in the online version of this article.

Figure S1. Specificity and sensitivity of different polyclonal antibodies raised in rabbits against recombinant piperine synthase (PS) and piperamide synthase (PAS).

Figure S2. Specificity of purified polyclonal PS and PAS antibodies against crude black pepper protein preparation.

Figure S3. PS and PAS signals of black pepper cells of the fruits embedded in Technovit 7100.

Figure S4. Piperamides in isolated root cells.

Figure S5. Piperine analysis of germinating black pepper seedlings.

OPEN RESEARCH BADGE

This article has earned an Open Data badge for making publicly available the digitally-shareable data necessary to reproduce the reported results. The data is available at (DOI) 10.22000/607.

REFERENCES

Arce-Rodríguez, M.L. & Ochoa-Alejo, N. (2019) Biochemistry and molecular biology of capsaicinoid biosynthesis: recent advances and perspectives. *Plant Cell Reports*, **38**, 1017–1030. Available from: https://doi.org/10.1007/s00299-019-02406-0

Baldwin, J.W. & Whitehead, S. (2015) Fruits secondary compounds mediate the retention time of seeds in the guts of neotropical fruit bats. *Oecologia*, **177**, 453–466. Available from: https://doi.org/10.1007/s00442-014-3096-2

Bay-Hurtado, F., Abreu-Lima, R., Fabiélen Teixiera, L., do Carmo Freire Silva, I., Bay, M., Soares Azevedo, M. *et al.* (2016) Antioxidant activity and characterization of the essential oil from the roots of *Piper marginatum* Jacq. *Ciência e Natura*, **38**, 1504–1511.

Beaudoin, G.A.W. & Facchini, P.J. (2014) Benzylalkaloid biosynthesis in opium poppy. *Planta*, **240**, 19–32. Available from: https://doi.org/10.1007/s00425-014-2056-8

Brillouet, J.M., Verdeil, J.L., Odoux, E., Lertaux, M., Grisoni, M. & Conéjero, G. (2014) Phenol homeostasis is ensured in vanilla fruit by storage under solid form in a new chloroplast-derived organelle, the phenyloplast. *Journal of Experimental Botany*, **65**, 2427–2435. Available from: https://doi.org/10.1093/jxb/eru126

Caterina, M.J., Schumacher, M.A., Tominago, M., Rosen, T.A., Levine, J.D. & Julius, D. (1997) The capsaicin receptor: a heat-activated ion channel in the pain pathway. *Nature*, **389**, 816–824. Available from: https://doi.org/10.1038/39807

Chandra, P., Bajpai, V., Srivastva, M., Kumar, K.B.R. & Kumar, B. (2004) Metabolic profiling of *Piper* species by direct analysis using real time mass spectrometry combined with principal component analysis. *Analytical Methods*, **6**, 4234–4239. Available from: https://doi.org/10.1039/C4AY00246F

Choi, Y. H., van Spronsen, J., Dai, Y., Verberne, M., Hollmann, F., Arends, I.W.C.E. *et al.* (2011) Are natural deep eutectic solvents the missing link in understanding cellular metabolism and physiology? *Plant Physiology*, **156**, 1701–1705. Available from: https://doi.org/10.1104/pp.111.178426

Dai, Y., Verpoorte, R. & Choi, Y.H. (2014) Natural deep eutectic solvents providing enhanced stability of natural colorants from safflower (*Carthamus tinctorius*). *Food Chemistry*, **159**, 116–121. https://doi.org/10.1016/j.foodchem.2014.02.155

Dastmalchi M., Chang, L., Chen, R. Yu, L., Chen, X., Hagel, J.M. *et al.* (2019) Purine permease-type benzylisoquinoline alkaloid transporters in opium poppy. *Plant Physiology*, **181**, 916–933. Available from: https://doi.org/10.1104/pp.19.00565.

D'Auria, J.C., Cheng, F. & Pichersky, E. (2002) Characterization of an acyltransferase capable of synthesizing benzylbenzoate and other volatile esters in flowers and damaged leaves of *Clarkia breweri*. *Plant Physiology*, **130**, 466–476. Available from: https://doi.org/10.1104/pp.006460

Debnath, S. & Mishra, J. (2020) Understanding the intrinsic fluorescence in piperine in microheterogenous media: partitioning and loading studies. *New Journal of Chemistry*, **44**, 8317–8324. Available from: https://doi.org/10.1039/d0nj00770f

Dyer, L.A., Dodson, C.D., Stireman III, J.O., Tobler, M.A., Smilanich, A.M., Fincher, R.M. *et al.* (2003) Synergistic effect of three piper amides on generalist and specialist herbivores. *Journal of Chemical Ecology*, **29**, 2499–2514. Available from: https://doi.org/10.1023/A:1026310001958

Fraser, C.M. & Chapple, C. (2011) The phenylpropanoid pathway in Arabidopsis. *Arabidopsis*, **9**, e0152. Available from: https://doi.org/10.1199/tab.0152

Fujiwake, H., Iwai, T. & Iwai, K. (1980) Intracellular localization of capsaicinoids and its analogues in *Capsicum* fruit II. The vacuole as the intracellular accumulation site of capsaicinoid in protoplast of *Capsicum* fruit. *Plant & Cell Physiology*, **21**, 1023–1030. Available from: https://doi.org/10.1093/oxfordjournals.pcp.a076070

Geisler, J. & Gross, G.G. (1990) The biosynthesis of piperine in *Piper nigrum*. *Phytochemistry*, **29**, 489–492. Available from: https://doi.org/10.1016/0031-9422(90)85102-L

Goebel-Stengel, M., Stengel, A., Tache, I. & Reeve, J.R. (2012) The importance of using the optimal plastic and glassware in studies involving peptides. *Analytical Biochemistry*, **414**, 38–46. Available from: https://doi.org/10.1016/j.ab.2011.02.009

Gordo, S.M., Pinheiro, D.G., Moreira, E.C.O., Rodrigues, S.M., Poltronieri, M.C., de Lemos, O.F. *et al.* (2012) High-throughput sequencing of black pepper root transcriptome. *BMC Plant Biology*, **12**, 168. Available from: https://doi.org/10.1186/1471-2229-12-168

Gorgani, L., Mohammadi, M., Najafpour, G.D. & Nikzad, M. (2017) Piperine – the bioactive compound from black pepper: from isolation to medicinal formulations. *Comprehensive Reviews in Food Science and Food Safety*, **16**, 124–140. Available from: https://doi.org/10.1111/1541-4337.12246

Hao, C., Xia, Z., Fan, R., Tan, L., Hu, L., Wu, B. *et al.* (2016) De novo transcriptome sequencing of black pepper (*Piper nigrum* L.) and an analysis of genes involved in phenylpropanoid metabolism in response to *Phytophthora capsici*. *BMC Genomics*, **17**, 1–14. Available from: https://doi.org/10.1186/s12864-016-3155-7

Hartmann, T., Ehmke, A., Eilert, U., von Borstel, K. & Theuring, C. (1989) Sites of synthesis, translocation and accumulation of pyrrolizidine

alkaloid N-oxides in *Senecio vulgaris* L. *Planta*, **177**, 98–107. Available from: https://doi.org/10.1007/BF00392159

Hu, L., Zu, Z., Wang, L., Fan, R., Yuan, D., Wu, B. *et al.* (2019) The chromosome scale reference genome of black pepper provides insight into piperine biosynthesis. *Nature Communications*, **10**, 4712. Available from: https://doi.org/10.1371/journal.pone.0129822

Irmer, S., Podzun, N., Langel, D., Heidemann, F., Kaltenegger, E., Schemmerling, B. *et al.* (2015) New aspect of plant-rhizobia interaction: alkaloid biosynthesis in *crotalaria* depends on nodulation. *Proceedings of the National Academy of Sciences of the United States of America*, **112**, 4164–4169. Available from: https://doi.org/10.1073/pnas.1423457112

Jelesko, J.G. (2012) An expanding role of purine uptake permase-like transporters in plant secondary metabolism. *Frontiers in Plant Science*, **3**, 78. Available from: https://doi.org/10.3389/fpls.2012.00078

Jin, Z., Wungsintaweekul, J., Kim, S.H., Kim, J.H., Shin, Y., Ro, D.K. *et al.* (2020). 4-Coumarate:coenzyme a ligase isoform 3 from *Piper nigrum* (Pn4CL3) catalyzes the CoA thioester formation of 3,4-methylenedioxycinnamic and piperic acids. *Biochemistry Journal*, **477**, 61–74. Available from: https://doi.org/10.1042/BCJ20190527

Kapoor, I.P.S., Singh, G., Singh, B., De Heluani, C.S., De Lampasona, M.P. & Catalan, C.A.N. (2009) Chemistry and in vitro antioxidant activity of volatile oil and oleoresins of black pepper (*Piper nigrum*). *Journal of Agricultural and Food Chemistry*, **57**, 5358–5364. Available from: https://doi.org/10.1021/jf900642x

Kato, M.J. & Furlan, M. (2007) Chemistry and evolution of the Piperaceae. *Pure and Applied Chemistry*, **79**, 529–538. Available from: https://doi.org/10.1351/pac200779040529

Knudsen, C., Bavishi, K., Viborg, K.M., Drew, D.P., Simonsen, H.T., Motavia, M.S. *et al.* (2020) Stabilization of dhurrin biosynthetic enzymes from *Sorghum bicolor* using a natural deep eutectic solvent. *Phytochemistry*, **170**, 112214. Available from: https://doi.org/10.1016/j.phytochem.2019.112214

Knudsen, C., Gallage, N.J., Hansen, C.C., Møller, B.L. & Laursen, T. (2018) Dynamic metabolic solutions to the sessile lifestyle of plants. *Natural Product Reports*, **35**, 1140–1155. Available from: https://doi.org/10.1039/C8NP00037A

Koroleva, O.A., Gibson, T.M., Cramer, R. & Stain, C. (2010) Glucosinolate-accumulating S-cells in Arabidopsis leaves and flower stalks undergo programmed cell death at early stages of differentiation. *The Plant Journal*, **64**, 456–469. Available from: https://doi.org/10.1111/j.1365-313X.2010.04339.x

Kulagina, N., Méteignier, L.-V., Papon, N., O'Connor, S.E. & Courdavault, V. (2022) More than a *Catharanthus* plant: a multicellular and pluri-organelle alkaloid-producing factory. *Current Opinion in Plant Biology*, **67**, 102200. Available from: https://doi.org/10.1016/j.pbi.2022.102200

Lang, M., Stober, F. & Lichtenthaler, H.K. (1991) Fluorescence emission spectra of plant leaves and plant constituents. *Radiation and Environmental Biophysics*, **30**, 333–347. Available from: https://doi.org/10.1007/BF01210517

Laursen, T., Borch, J., Knudsen, C., Bavishi, K., Torta, F., Martens, H.J. *et al.* (2016) Characterization of a dynamic metabolon producing the defense compound dhurrin in sorghum. *Science*, **354**, 890–893. Available from: https://doi.org/10.1126/science.aag2347

Majovsky, P., Naumann, C., Lee, C.W., Lassowskat, I., Trujillo, M., Dissmeyer, N. & Hoehenwarter, W. (2014) Targeted proteomics analysis of protein degradation in plant signaling on an LTQ-orbitrap mass spectrometer. *Journal of Proteome Research*, **13**, 4246–4258. Available from: https://doi.org/10.1021/pr500164j

Meghwal, M. & Goswami, T. (2013) *Piper nigrum* and piperine: an update. *Phytotherapy Research*, **27**, 1121–1130. Available from: https://doi.org/10.1002/ptr.4972

Møller, B.L. & Conn, E. (1980) The biosynthesis of cyanogenic glucosides in higher plants. Channeling of intermediates in dhurrin biosynthesis by a microsomal system from *Sorghum bicolor* (Linn) Moench. *The Journal of Biological Chemistry*, **255**, 3049–3056. Available from: https://doi.org/10.1016/S0021-9258(19)85850-7

Moreira, E.C.O., Pinheiro, D.G., Gordo, S.M.C., Rodrigues, S.M., Pessoa, E., Schaller, H. *et al.* (2017) Transcriptional profiling by RNA sequencing of black pepper (*Piper nigrum L.*) roots infected by *Fusarium solani* f. sp. *piperis*. *Acta Physiologiae Plantarum*, **39**, 239. Available from: https://doi.org/10.1007/s11738-017-2538-y

Morita, M., Shitan, N., Sawada, K., van Montagu, M.C.M., Inze, D., Rischer, H. *et al.* (2009) Vacuolar transport of nicotine is mediated by a multidrug and toxic compound extrusion (MATE) transporter in *Nicotiana tabacum*. *Proceedings of the National Academy of Sciences of the United States of America*, **106**, 2447–2452. Available from: https://doi.org/10.1073/pnas.0812512106

Otani, N., Shitan, N., Sakai, K., Martinoia, E., Sato, F. & Yazaki, K. (2005) Characterization of vacuolar transport of the endogenous alkaloid berberine in *Coptis japonica*. *Plant Physiology*, **138**, 1939–1946. Available from: https://doi.org/10.1104/pp.105.064352

Ozber, N. & Facchini, P.J. (2022) Phloem-specific localization of benzylisoquinoline alkaloid metabolism in opium poppy. *Journal of Plant Physiology*, **271**, 153641. Available from: https://doi.org/10.1016/j.jplph.2022.153641.

Pavoković, D., Kospić, K., Panić, M., Redovniković, I.R. & Bubalo, M.C. (2020) Natural deep eutectic solvents are viable solvents for plant cell culture-assisted stereoselective biosynthesis. *Process Biochemistry*, **93**, 69–76. Available from: https://doi.org/10.1016/j.procbio.2020.03.020

Pičmanová, M., Neilson, E. H., Motawia, M. S., Olsen, C. E., Agerbirk, N., Gray, C. J. *et al.* (2015). A recycling pathway for cyanogenic glycosides evidenced by the comparative metabolic profiling in three cyanogenic plant species. *The Biochemical Journal*, **469**, 375–389. Available from: https://doi.org/10.1042/BJ20150390

Rodziewicz, P., Loroch, S., Marczak, L., Sickman, A. & Kayser, O. (2019) Cannabinoid synthases and osmoprotective metabolites accumulate in the exudates of *Cannabis sativa* L. glandular trichomes. *Plant Science*, **284**, 108–116. Available from: https://doi.org/10.1016/j.plantsci.2019.04.008

Schnabel, A., Athmer, B., Manke, K., Schumacher, F., Cotinguiba, F. & Vogt, T. (2021) Identification and characterization of piperine synthase from black pepper*Piper nigrum* L. *Communications Biology*, **4**, 445. Available from: https://doi.org/10.1038/s42003-021-01967-9

Schnabel, A., Cotinguiba, F., Athmer, B. & Vogt, T. (2021) *Piper nigrum* CYP719A37 catalyzes the decisive methylenedioxy bridge formation in piperine biosynthesis. *Plants*, **10**, 128. Available from: https://doi.org/10.3390/plants10010128

Schnabel, A., Cotinguiba, F., Athmer, B., Yang, C., Westermann, B., Schaks, A. *et al.* (2020) Identification and functional characterization of a specific piperic acid CoA ligase from black pepper (*Piper nigrum* L.) immature fruits. *Plant Journal*, **102**, 569-581. Available from: https://doi.org/10.1111/tpj.14652

Schulz, H., Baranska, M., Quilitzsch, R., Schütze, W. & Lösing, G. (2005) Characterization of peppercorn, pepper oil, and pepper oleoresin by vibrational spectroscopy methods. *Journal of Agricultural and Food Chemistry*, **53**, 3358–3363. Available from: https://doi.org/10.1021/jf048137m

Scott, I.M., Jensen, H.R., Philogène, B.J.R. & Arnason, J.T. (2008) A review of *piper* spp. (Piperaceae) phytochemistry, insecticidal activity and mode of action. *Phytochemistry Reviews*, **7**, 65–75. Available from: https://doi.org/10.1021/jf048305a

Semler, U. & Gross, G.G. (1987) Distribution of piperine in vegetative parts of *Piper nigrum*. *Phytochemistry*, **27**, 1566–1567. Available from: https://doi.org/10.1016/0031-9422(88)80249-8

Shirakawa, M., Tanita, M. & Ito, T. (2021) The differentiation of idioblast myrosin cells: similarities to guard and vascular cells. *Frontiers in Plant Science*, **12**, 829541. Available from: https://doi.org/10.3389/fpls.2021/829541

Spring, F.S. & Stark, J. (1950) Piperettine from *Piper nigrum*: its isolation, identification, and synthesis. *Journal of the Chemical Society (London)*, 1177–1180.

Spurr, A.R. (1969) A low-viscosity epoxy resin embedding medium for electron microscopy. *Journal of Ultrastructure Research*, **26**, 31–43. Available from: https://doi.org/10.1016/S0022-5320(69)90033-1

Stewart, C., Mazourek, M., Stellari, G.M., O'Connell, M. & Jahn, M. (2007) Genetic control of pungency in *C. chinense* via the *Pun1* locus. *Journal of Experimental Botany*, **58**, 979–991. Available from: https://doi.org/10.1093/jxb/erl243

St-Pierre, B., Vazquez-Flota, F.A. & De Luca, V. (1999) Multicellular compartmentation of *Catharanthus roseus* alkaloid biosynthesis predicts intercellular translocation of a pathway intermediate. *The Plant Cell*, **11**, 887–900. Available from: https://doi.org/10.1105/tpc.11.5.887

Suire, C., Bouvier, F., Backhaus, R.A., Bégu, D., Bonneu, M. & Camara, B. (2000) Cellular localization of isoprenoid biosynthetic enzymes in *Marchantia polymorpha*: uncovering a new role of oil bodies. *Plant Physiology*, **124**, 971–978. Available from: https://doi.org/10.1104/pp.124.3.971

Suresh, V.K., Mahesha, H.G., Rao, A.G.A. & Srinivasan, A. (2007) Binding of bioactive biochemical piperine with human serum albumin; a spectrophotometric study. *Biopolymers*, **86**, 265–275. Available from: https://doi.org/10.1002/bip.20735

Tanaka. Y., Watachi, M., Nemoto, W., Goto, T., Toshida, Y., Yasuda, K.I. *et al.* (2021) Capsaicinoid biosynthesis in the pericarp of chili pepper fruit is associated with a placental septum-like transcriptome profile and tissue structure. *Plant Cell Reports*, **40**, 1859–1874. Available from: https://doi.org/10.1007/s00299-021-02750-0

Uzaki, M., Yamamoto, K., Murakami, A., Fuji, Y., Ohnishi, M., Ishizaki, K. *et al.* (2022) Differential regulation of fluorescent alkaloid metabolism between idioblast and lacticifer cells during leaf development in *Catharanthus roseus* seedlings. *Journal of Plant Research*, **1–11**, 473–483. Available from: https://doi.org/10.1007/s10265-022-01380-1

Wei, K., Li, W., Koike, K., Pei, Y., Chen, Y. & Nikaido, T. (2004) New amide alkaloids from the roots of black pepper. *Journal of Natural Products*, **676**, 1005–1009. Available from: https://doi.org/10.1021/np030475e

Wessel, D. & Flügge, U.I. (1984) A method for the quantitative recovery of protein in dilute solution in the presence of detergents and lipids. *Analytical Biochemistry*, **138**, 141–143. Available from: https://doi.org/10.1016/0003-2697(84)90782-6

Yamamoto, K., Takahashi, K., Caputi, L., Mizuno, H., Rodriguez-Lopez, C.E., Iwasaki, T. *et al.* (2019) The complexity of intercellular localization of alkaloids revealed by single-cell metabolomics. *The New Phytologist*, **224**, 848–859. Available from: https://doi.org/10.1111/nph.16138

Yu, F. & de Luca, V. (2014) ATP-binding cassette transporter controls leaf surface secretion of anticancer drug components in *Catharanthus roseus*. *Proceedings of the National Academy of Sciences*, **110**, 15830–15835. Available from: https://doi.org/10.1073/pnas.1307504110